Supplementary Information

Molecular Modification in Hybrid Material induces Multiple Ferroic Ordering

Jia-Xun Li,[a] Hao-Ran Chen,[a] Zhi-Long Li,[a] Bo Zhuang,[a] Meng-Meng Lun*[c] Zhi-Xu Zhang*[b] and Da-Wei Fu*[a,b]

[a] *Ordered Matter Science Research Center, Jiangsu Key Laboratory for Science and Applications of Molecular Ferroelectrics, Southeast University, Nanjing 211189, China.*

[b] *Institute for Science and Applications of Molecular Ferroelectrics, Key Laboratory of the Ministry of Education for Advanced Catalysis Materials, Zhejiang Normal University, Jinhua, Zhejiang 321004, China*

[c] *School of Electronics and Information, Zhengzhou University of Light Industry, Zhengzhou 450000, China*

Synthesis of TPM, TPAM, and CTPAM

A mixture of trimethylamine (0.1 mol) and each of the three precursors 1-Bromo-2-Methylpropane, 3-Bromo-2-methylpropene, and 2,3-Dichloro-1-Propene (0.1 mol each, respectively) was dissolved separately in 50 mL of ethyl acetate and stirred at room temperature for 1 h. The resulting solutions were subsequently transferred to a constant-temperature environment at 323 K and maintained for 24 h. After rotary evaporation, three white powder products were obtained and designated as TPM, TPAM, and CTPAM, respectively.

Detailed methods of measurements

Variable-Temperature Single-crystal XRD

Single-crystal X-ray diffraction data were obtained using a Rigaku Saturn 724 diffractometer with Mo Kα radiation (λ = 0.71073 Å). The structure data of the variable temperature crystal was solved using the direct method, and the crystal structure was analyzed and refined using SHELXL software. Import the CIF file generated by SHELXL software into DIAMOND to plot the corresponding cell diagram. These X-ray crystal structures have been stored at the Cambridge Crystallography Data Center (storage number CCDC 2512977-2512980, 2514785) and are available free of charge from CCDC at www.ccdc.cam.ac.uk/getstructures.

DSC Measurement

Grind the crystal sample into powder, dry it, and weigh approximately 5–10 milligrams of powder into an aluminum crucible. Subsequently, under a nitrogen atmosphere, use the NETZSCH DSC 214 polymer analyzer to uniformly heat and cool the sample at a temperature ramp rate of 20 K min^{-1} within the preset temperature program.

Dielectric Measurement

Press the powder sample into a sheet-like specimen approximately 5 mm^2 in area and 0.5 mm thick. Connect the sheet-like specimen to both ends of the electrodes using copper wire and conductive silver paste to form a capacitor. Measure the complex dielectric constant at different temperatures and frequencies using the Tonghui TH 2828 A instrument under 1 V AC voltage.

SHG Measurement

The SHG measurement of powder samples was primarily conducted using an FLS 920, Edinburgh Instruments, employing a low-divergence, unexpanded laser beam(pulse: Nd:YAG,wavelength: 1064 nm,peak power: 1.6 MW,repetition rate: 10 Hz,pulse duration: 5 ns) within a defined temperature cycle.

Ferroelectric hysteresis loop characterizations

The polarization versus electric field (P–E) hysteresis loop test for single crystals employs the Sawyer-Tower method.

PXRD Measurement

Powder X-ray diffraction (PXRD) measurements were performed on a Rigaku SmartLab SE X-ray diffractometer. Diffraction patterns were recorded in the 2θ range of 5–50° with a step size of 0.02°. Temperature-programmed powder X-ray diffraction patterns were obtained across the 298–383 K temperature range by setting the heating and cooling program.

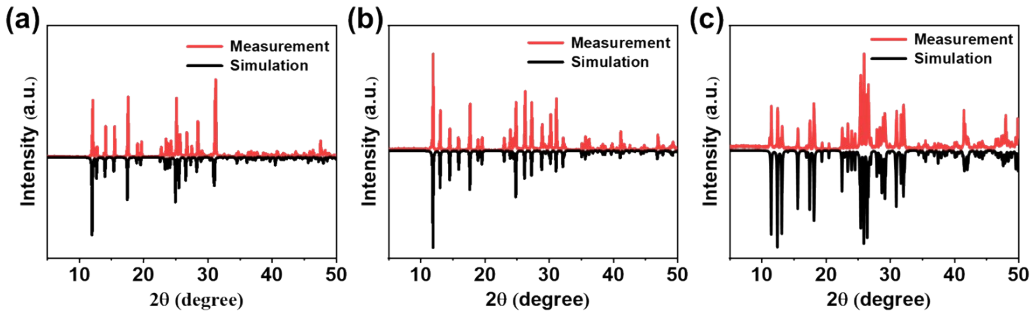

Fig. S1 The measured and simulated PXRD patterns of TPM-$FeBr_4$, TPAM-$FeBr_4$, and CTPAM-$FeBr_4$

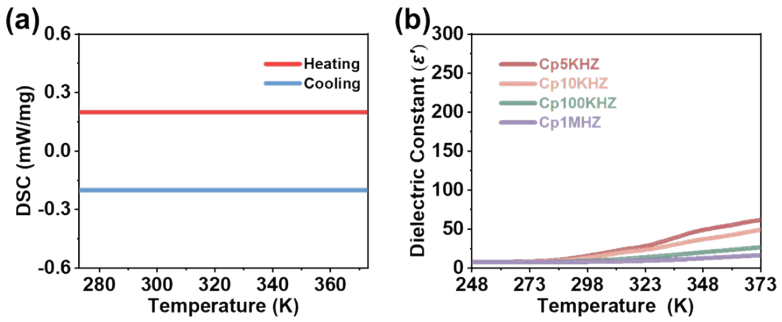

Fig. S2 (a) DSC curves of TPM-$FeBr_4$ in a heating-cooling cycle, (b) Temperature dependence of the real part (ε') of TPM-$FeBr_4$ at different frequencies.

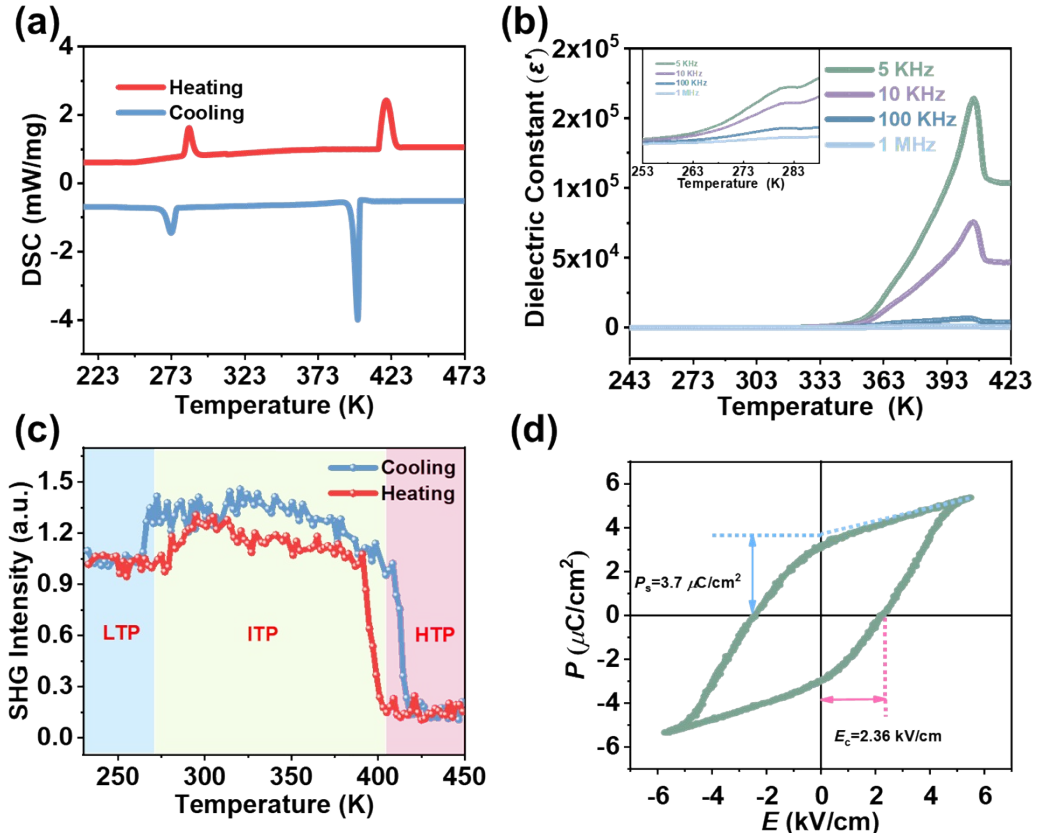

Fig. S3 (a) DSC curves of TPAM-$FeBr_4$ in a heating-cooling cycle. (b) Temperature dependence of the real part (ε') of TPAM-$FeBr_4$ at different frequencies. (c) Temperature-dependent SHG response of TPAM-$FeBr_4$. (d) P-V hysteresis loop of CTPAM-$FeBr_4$ at room temperature.

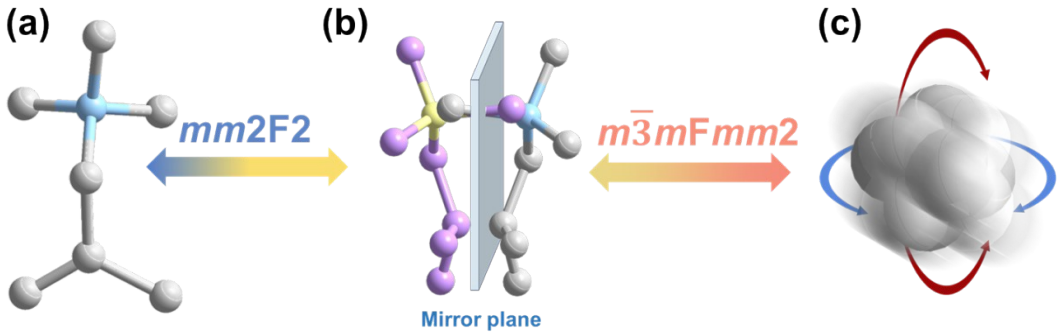

Fig. S4 Structure of organic cations when TPAM-$FeBr_4$ crystallizes in the LTP (a) , ITP (b) , HTP (c).

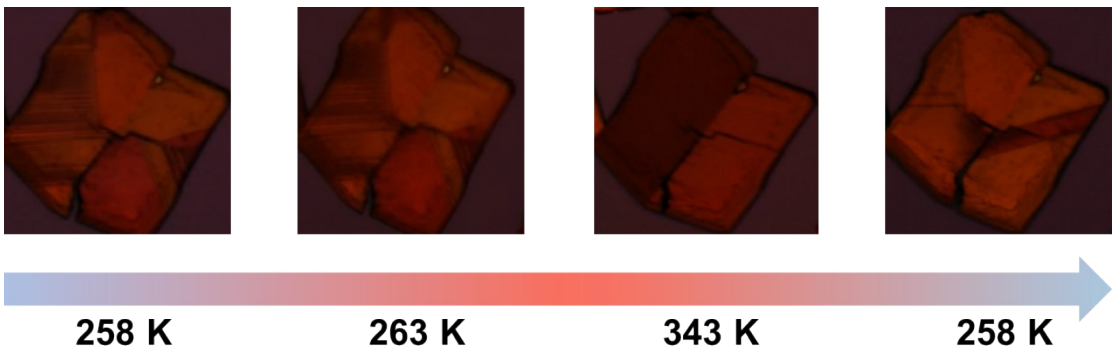

Fig. S5 The evolution of ferroelastic domain of TPAM-$FeBr_4$ during continuous heating and cooling proce ss.

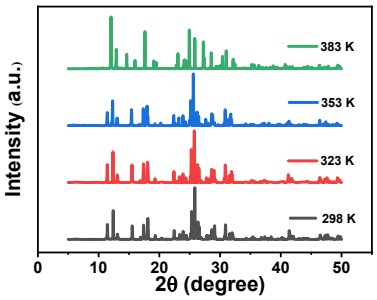

Fig. S6 Variable-temperature PXRD spectra of CTPAM-$FeBr_4$.

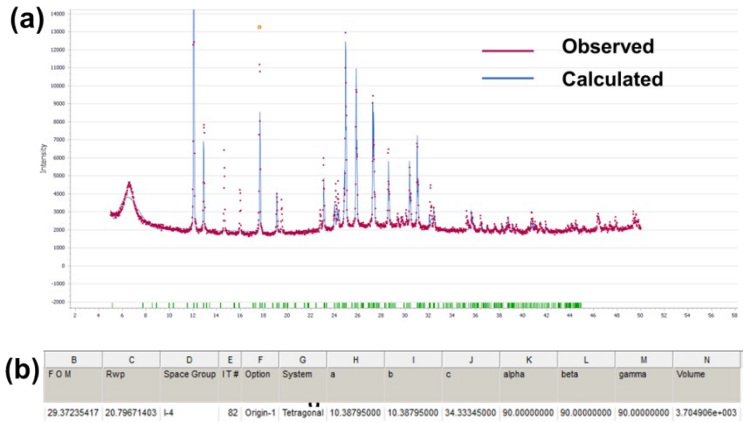

Figure S7 Pattern of powder X-ray diffraction refined (a) and solution (b) of CTPAM-$FeBr_4$ at 383 K.

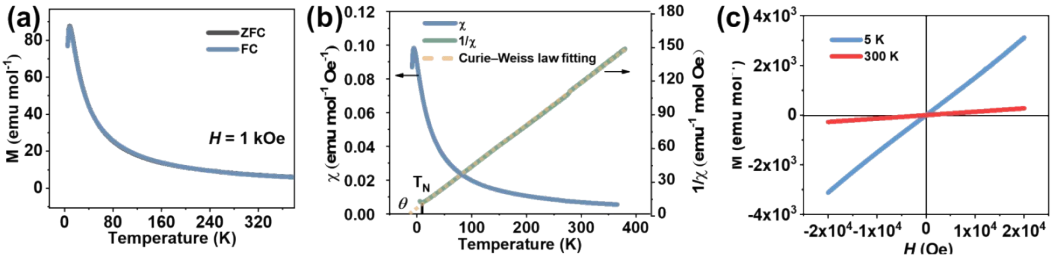

Fig. S8 (a) Temperature-dependent magnetization intensity *M-T* of TPAM-$FeBr_4$. (b) Temperature-depende nt magnetization *c* (left axis) and inverse magnetizatio c^{-1} (right axis) for TPAM-$FeBr_4$. (c) Magnetic field-dependent *M-H* loops before and after the magnetic transition of TPAM-$FeBr_4$.

Table S1 Crystal data for TPM-$FeBr_4$ (293 K) and CTPAM-$FeBr_4$ (273 K).

	TPM-$FeBr_4$ (293 K)	CTPAM-$FeBr_4$ (273 K)
Empirical formula	$C_7H_{18}Br_4FeN$	$C_6H_{14}Br_4ClFeN$
Formula weight	491.71	511.12
Space group	$Cmc2_1$ (36)	$P2_1$ (4)
***a* (Å)**	9.081(3)	7.1975(11)

***b* (Å)**	12.653(3)	13.488(2)
***c* (Å)**	13.959(5)	7.8050(15)
α (°)	90	90
β (°)	90	98.685(11)
γ (°)	90	90
Volume (Å^3)	1604.0(8)	749.0(2)
Z	4	2
***F*(000)**	932	480
R_{int}	0.1550	0.0663
R_1	0.1451	0.0768
wR_2	0.2975	0.1901
GOF	1.058	1.033

Table S2 Crystal data for TPAM-$FeBr_4$ at 263 K, 303 K and 423 K.

	TPAM-$FeBr_4$ (263 K)	TPAM-$FeBr_4$ (303K)	TPAM-$FeBr_4$ (423 K)
Empirical formula	$C_7H_{17}Br_4FeN$	$C_7H_{16}Br_4FeN$	C_7Br_6Fe
Formula weight	490.71	489.70	619.38
Space group	$P2_1$ (4)	$Cmc2_1$ (36)	$Pm\bar{3}m$ (221)
***a* (Å)**	7.292(2)	9.386(4)	7.523(2)
***b* (Å)**	13.559(4)	12.203(6)	7.523(2)
***c* (Å)**	7.790(2)	13.615(7)	7.523(2)
α (°)	90	90	90
β (°)	99.597(7)	90	90
γ (°)	90	90	90
Volume (Å^3)	759.4(4)	1559.4(13)	425.8(3)
Z	2	4	1
***F*(000)**	464	924	278
R_{int}	0.1323	0.1314	0.0858
R_1	0.1337	0.1421	0.0734
wR_2	0.1836	0.2853	0.1437
GOF	1.012	1.049	1.069

Table S3 The bond lengths (Å) and angles (°) of TPM-$FeBr_4$ at 263 K.

Atom–Atom	Length [Å]	Atom–Atom–Atom	Angle [°]
Br01–Fe1	2.322(3)	Br01–Fe1–Br02	109.52(11)
Br02–Fe1	2.348(3)	Br01–Fe1–Br04	110.30(8)
Fe1–Br04	2.3497(18)	Br01–Fe1–Br04$^{\#1}$	110.31(8)
Fe1–Br04$^{\#1}$	2.3497(18)	Br02–Fe1–Br04$^{\#1}$	109.20(8)
N005–C3	1.4300(7)	Br02–Fe1–Br04	109.20(8)
N005–C3$^{\#1}$	1.4300(7)	Br04$^{\#1}$–Fe1–Br04	108.29(11)
N005–C1	1.4300(9)	C3–N005–C3$^{\#1}$	85.86(7)

N005–C2	1.475(9)	$C3^{\#1}$–N005–C2	127.7(4)
N005–C4	1.448(8)	C3–N005–C2	108.6(4)
C10–H10	0.9800	C3–N005–C4	109.9(4)
C10–C1	1.5400(8)	$C3^{\#1}$–N005–C4	26.3(4)
$C10–C0^{\#1}$	1.5400(8)	$C1–N005–C3^{\#1}$	111.54(14)
C10–C0	1.5400(8)	C1–N005–C3	111.54(14)
C3–H3A	0.9600	C1–N005–C2	108.8(4)
C3–H3B	0.9600	C1–N005–C4	110.2(4)
C3–H3C	0.9601	C4–N005–C2	107.7(6)
C1–H1A	0.9700	C1–C10–H10	102.2
C1–H1B	0.9700	C1–C10–C0	118.30(6)
C0–H0A	0.9602	$C1–C10–C0^{\#1}$	118.30(6)
C0–H0B	0.9601	C0–C10–H10	102.2
C0–H0C	0.9597	$C0^{\#1}$–C10–H10	102.2
C2–H2A	0.9601	$C0–C10–C0^{\#1}$	110.26(8)
C2–H2B	0.9600	N005–C3–H3A	109.1
C2–H2C	0.9601	N005–C3–H3B	110.1
C4–H4A	0.9602	N005–C3–H3C	109.2
C4–H4B	0.9601	H3A–C3–H3B	109.5
C4–H4C	0.9600	H3A–C3–H3C	109.5
		H3B–C3–H3C	109.5
		N005–C1–C10	149.22(9)
		N005–C1–H1A	99.4
		N005–C1–H1B	99.4
		C10–C1–H1A	99.4
		C10–C1–H1B	99.4
		H1A–C1–H1B	104.0
		C10–C0–H0A	109.3
		C10–C0–H0B	110.4
		C10–C0–H0C	108.7
		H0A–C0–H0B	109.5
		H0A–C0–H0C	109.5
		H0B–C0–H0C	109.5
		N005–C2–H2A	109.2
		N005–C2–H2B	110.3
		N005–C2–H2C	109.0
		H2A–C2–H2B	109.5
		H2A–C2–H2C	109.5
		H2B–C2–H2C	109.5
		N005–C4–H4A	110.3
		N005–C4–H4B	109.4
		N005–C4–H4C	108.7
		H4A–C4–H4B	109.5
		H4A–C4–H4C	109.5

		H4B–C4–H4C	109.5

Table S4 The bond lengths (Å) and angles (°) of TPAM-$FeBr_4$ at 263 K.

Atom–Atom	Length [Å]	Atom–Atom–Atom	Angle [°]
Br3–Fe05	2.343(3)	Br2–Fe05–Br3	108.26(11)
Br2–Fe05	2.331(3)	Br1–Fe05–Br3	109.88(13)
Br1–Fe05	2.323(3)	Br1–Fe05–Br2	108.60(12)
Br4–Fe05	2.322(3)	Br4–Fe05–Br3	109.08(12)
N1–C1	1.51(2)	Br4–Fe05–Br2	109.16(13)
N1–C5	1.48(3)	Br4–Fe05–Br1	111.79(13)
N1–C7	1.49(3)	C5–N1–C1	110.8(15)
N1–C6	1.45(3)	C5–N1–C7	108.1(19)
C3–H3	0.9800	C7–N1–C1	108.5(16)
C3–C1	1.48(3)	C6–N1–C1	109.5(15)
C3–C2	1.412(19)	C6–N1–C5	109(2)
C3–C4	1.48(3)	C6–N1–C7	111(2)
C1–H1A	0.9700	C1–C3–H3	91.6
C1–H1B	0.9700	C2–C3–H3	91.6
C2–H2A	0.9600	C2–C3–C1	120.1(18)
C2–H2B	0.9600	C2–C3–C4	118.6(19)
C2–H2C	0.9600	C4–C3–H3	91.6
C5–H5A	0.9600	C4–C3–C1	121.1(16)
C5–H5B	0.9600	N1–C1–H1A	107.7
C5–H5C	0.9600	N1–C1–H1B	107.7
C4–H4A	0.9600	C3–C1–N1	118.5(13)
C4–H4B	0.9600	C3–C1–H1A	107.7
C4–H4C	0.9600	C3–C1–H1B	107.7
C7–H7A	0.9600	H1A–C1–H1B	107.1
C7–H7B	0.9600	C3–C2–H2A	109.5
C7–H7C	0.9600	C3–C2–H2B	109.5
C6–H6A	0.9600	C3–C2–H2C	109.5
C6–H6B	0.9600	H2A–C2–H2B	109.5
C6–H6C	0.9600	H2A–C2–H2C	109.5
		H2B–C2–H2C	109.5
		N1–C5–H5A	109.5
		N1–C5–H5B	109.5
		N1–C5–H5C	109.5
		H5A–C5–H5B	109.5
		H5A–C5–H5C	109.5
		H5B–C5–H5C	109.5
		C3–C4–H4A	109.5
		C3–C4–H4B	109.5
		C3–C4–H4C	109.5
		H4A–C4–H4B	109.5

H4A–C4–H4C	109.5
H4B–C4–H4C	109.5
N1–C7–H7A	109.5
N1–C7–H7B	109.5
N1–C7–H7C	109.5
H7A–C7–H7B	109.5
H7A–C7–H7C	109.5
H7B–C7–H7C	109.5
N1–C6–H6A	109.5
N1–C6–H6B	109.5
N1–C6–H6C	109.5
H6A–C6–H6B	109.5
H6A–C6–H6C	109.5
H6B–C6–H6C	109.5

Table S5 The bond lengths (Å) and angles (°) of TPAM-$FeBr_4$ at 303 K.

Atom–Atom	Length [Å]	Atom–Atom–Atom	Angle [°]
Br01–Fe02	2.324(6)	Br03–Fe02–Br01	109.7(3)
Fe02–Br03	2.306(7)	Br03–Fe02–Br04	110.7(2)
Fe02–Br04$^{\#1}$	2.318(5)	Br03–Fe02–Br04$^{\#1}$	110.7(2)
Fe02–Br04	2.318(5)	Br04$^{\#1}$–Fe02–Br01	108.8(2)
C5–C4	1.4669(7)	Br04–Fe02–Br01	108.8(2)
C5–C6	1.3581(5)	Br04–Fe02–Br04$^{\#1}$	108.0(3)
C5–C7	1.4699(4)	C4–C5–C7	129.102(7)
N006–C4	1.4306(6)	C6–C5–C4	124.75(2)
N006–C1	1.4312(4)	C6–C5–C7	105.86(3)
N006–C2	1.4301(6)	C4–N006–C1	110.31(3)
N006–C3	1.4311(6)	C4–N006–C3	109.223(10)
C4–H4A	0.9700	C2–N006–C4	109.516(19)
C4–H4B	0.9700	C2–N006–C1	109.02(2)
C6–H6A	0.9300	C2–N006–C3	108.952(15)
C6–H6B	0.9300	C3–N006–C1	109.80(3)
C1–H1A	0.9600	C5–C4–H4A	109.7
C1–H1B	0.9599	C5–C4–H4B	109.7
C1–H1C	0.9600	N006–C4–C5	110.047(19)
C7–H7A	0.9600	N006–C4–H4A	109.7
C7–H7B	0.9599	N006–C4–H4B	109.7
C7–H7C	0.9601	H4A–C4–H4B	108.2
C2–H2A	0.9600	C5–C6–H6A	120.0
C2–H2B	0.9601	C5–C6–H6B	120.0
C2–H2C	0.9600	H6A–C6–H6B	120.0
C3–H3A	0.9599	N006–C1–H1A	119.2
C3–H3C	0.9602	N006–C1–H1B	82.7
C3–H3B	0.9600	N006–C1–H1C	122.1

		H1A–C1–H1B	109.5
		H1A–C1–H1C	109.5
		H1B–C1–H1C	109.5
		C5–C7–H7A	109.5
		C5–C7–H7B	120.7
		C5–C7–H7C	97.3
		H7A–C7–H7B	109.5
		H7A–C7–H7C	109.5
		H7B–C7–H7C	109.5
		N006–C2–H2A	122.1
		N006–C2–H2B	95.3
		N006–C2–H2C	109.9
		H2A–C2–H2B	109.5
		H2A–C2–H2C	109.5
		H2B–C2–H2C	109.5
		N006–C3–H3A	136.6
		N006–C3–H3C	93.6
		N006–C3–H3B	95.7
		H3A–C3–H3C	109.5
		H3A–C3–H3B	109.5
		H3C–C3–H3B	109.5

Table S6 The bond lengths (Å) and angles (º) of CTPAM-$FeBr_4$ at 273 K.

Atom–Atom	**Length [Å]**	**Atom–Atom–Atom**	**Angle [°]**
Br1–Fe1	2.328(3)	Br1–Fe1–Br2	108.57(11)
Br2–Fe1	2.340(3)	Br1–Fe1–Br4	108.29(12)
Br3–Fe1	2.320(3)	Br3–Fe1–Br1	109.90(12)
Br4–Fe1	2.330(3)	Br3–Fe1–Br2	108.89(12)
Cl1–C2	1.69(2)	Br3–Fe1–Br4	111.51(13)
N1–C3	1.474(8)	Br4–Fe1–Br2	109.64(14)
N1–C4	1.470(8)	C4–N1–C3	113.0(17)
N1–C5	1.465(8)	C4–N1–C6	104.1(17)
N1–C6	1.472(8)	C5–N1–C3	116.1(14)
C3–H3A	0.9700	C5–N1–C4	111(2)
C3–H3B	0.9700	C5–N1–C6	105(3)
C3–C2	1.49(2)	C6–N1–C3	106(2)
C2–C1	1.514(8)	N1–C3–H3A	109.0
C4–H4A	0.9600	N1–C3–H3B	109.0
C4–H4B	0.9600	N1–C3–C2	113.1(14)
C4–H4C	0.9600	H3A–C3–H3B	107.8
C1–H1A	0.9300	C2–C3–H3A	109.0
C1–H1B	0.9300	C2–C3–H3B	109.0
C5–H5A	0.9598	C3–C2–Cl1	120.8(14)
C5–H5B	0.9601	C3–C2–C1	119.6(19)

C5–H5C	0.9601	C1–C2–Cl1	117.9(16)
C6–H6A	0.9600	N1–C4–H4A	109.5
C6–H6B	0.9601	N1–C4–H4B	109.5
C6–H6C	0.9600	N1–C4–H4C	109.5
		H4A–C4–H4B	109.5
		H4A–C4–H4C	109.5
		H4B–C4–H4C	109.5
		C2–C1–H1A	120.0
		C2–C1–H1B	120.0
		H1A–C1–H1B	120.0
		N1–C5–H5A	106.1
		N1–C5–H5B	111.4
		N1–C5–H5C	110.9
		H5A–C5–H5B	109.5
		H5A–C5–H5C	109.5
		H5B–C5–H5C	109.5
		N1–C6–H6A	107.9
		N1–C6–H6B	109.3
		N1–C6–H6C	111.1
		H6A–C6–H6B	109.5
		H6A–C6–H6C	109.5
		H6B–C6–H6C	109.5